Published in final edited form as:
Biochemistry. 2013 May 14; 52(19): . doi:10.1021/bi400109d.

Elucidating a Relationship between Conformational Sampling and Drug Resistance in HIV-1 Protease

Ian Mitchelle S. de Vera[†], **Adam N. Smith**[†], **Maria Cristina Dancel**[‡], **Xi Huang**[†], **Ben M. Dunn**[§], and **Gail E. Fanucci**[*,†]

[†]Department of Chemistry, P.O. Box 117200 University of Florida, Gainesville, FL 32611-7200

[‡]Mass Spectrometry Facility, Department of Chemistry, P.O. Box 117200 University of Florida, Gainesville, FL 32611-7200

[§]Department of Biochemistry and Molecular Biology, University of Florida College of Medicine Health Science Center, Gainesville, FL 32610-0245

Abstract

Enzyme targets in rapidly replicating systems, such as retroviruses, commonly respond to drug-selective pressure with mutations arising in the active site pocket that limit inhibitor effectiveness by introducing steric hindrance or by eliminating essential molecular interactions. However, these primary mutations are disposed to compromising pathogenic fitness. Emerging secondary mutations, which are often found outside of the binding cavity, may or can restore fitness while maintaining drug resistance. The accumulated drug-pressure selected mutations could have an indirect effect in the development of resistance, such as altering protein flexibility or the dynamics of protein-ligand interactions. Here, we show that accumulation of mutations in a drug-resistant variant, D30N/M36I/A71V, HIV-1 protease (HIV-1 PR) changes the fractional occupancy of the equilibrium conformational sampling ensemble. Correlations are made among populations of the conformational states; namely, closed-like, semi-open, and open-like, with inhibition constants, as well as kinetic parameters. Mutations that stabilize a closed-like conformation correlate with enzymes of lowered activity and with higher affinity for inhibitors, which is corroborated by a further increase in the fractional occupancy of the closed state upon addition of inhibitor or substrate-mimic. Cross resistance is found to correlate with combinations of mutations that increase the population of the open-like conformations at the expense of the closed-like state while retaining native-like occupancy of the semi-open population. These correlations suggest that at least three states are required in the conformational sampling model to establish the emergence of drug-resistance in HIV-1 PR. More importantly, these results shed light on a possible mechanism whereby mutations combine to impart drug resistance while maintaining catalytic activity.

The inhibition of enzymes through small molecules that compete with a substrate for the active site is a common clinical method for effective treatment of disease. However, the development of drug resistance in rapidly proliferating cells or pathogenic organisms through selective pressure, where the incorporation of random genetic mutations leads to the generation of an enzyme with amino acid substitutions, renders the drug molecule less effective.[1, 2] The emergence of primary mutations often results in a change in an amino acid whose structure interacts less favorably with the inhibitor by introducing steric hindrance or

[*]Corresponding author: (G. E. Fanucci) Tel.: + 1 352 392 2345; Fax: + 1 352 392 0872; fanucci@chem.ufl.edu.

Supporting Information Available

Characterization of MTSL-labeled HIV-1 protease by mass spectrometry and circular dichroism, along with complete DEER data processing and χ^2 error analysis are provided as supporting material. This material is available free of charge via the internet at http://pubs.acs.org.

by removing essential molecular interactions, such as charge stabilization or van der Waals contacts.[1, 2] In the case of competitive inhibition, these primary mutations also tend to alter the interactions of the enzyme with the substrate or product, thus negatively impacting enzyme efficiency and compromising fitness. The observed pattern of continued evolutionary mutations shows that secondary mutations (also referred to as compensatory mutations) recover fitness, while maintaining drug-resistance.[3]

An understanding of the molecular mechanism by which the accumulation of mutations impart these effects is important for the rational design of future generations of drugs.[4] In some enzymes, a clear rationale is illuminated through structural changes induced by the pattern of mutations, while in others, indirect effects such as changes in enzyme dynamics or protein-ligand dynamics are evoked.[2] Here, we elucidate how shifts in equilibrium conformational sampling can act as an “indirect” mechanism by which drug-pressure accumulated mutations alter enzyme kinetics and inhibitor susceptibility. Some proteins are known to sample multiple conformations, where interaction with a ligand or an inhibitor simply shifts the population to an already accessible state.[5-7] Specifically, our work focuses on mutation induced changes in the fractional occupancy of the conformational sampling ensemble as an “indirect” mechanism for drug-resistance in HIV-1 protease (HIV-1 PR).

HIV-1 PR, an aspartic protease that processes the *gag* and *gag-pol* viral polypeptides, is an attractive target for AIDS antiviral therapy[8] because of its central role in viral maturation.[9] Protease inhibitors (PIs) that target HIV-1 PR prevent the formation of infectious virions by blocking viral replication. PIs bind in the protease active site where the two flexible β-hairpin turns (aka *the flaps*) are folded over the inhibitor, giving a stable complex that prevents substrate access to the active site and subsequent processing.[10] The efficacy of currently available PIs is limited by the rapid emergence of mutations in HIV-1 PR, where changes in at least 38 out of 99 amino acid residues occur under the selective pressure of PI therapy, leading to lowered drug susceptibility.[11]

In HIV-1 PR, structural evidence clearly explains the effects that primary mutations in the active site pocket have on lowering inhibitor efficiency.[12] Secondary substitutions, on the other hand, often appear at locations outside the active site pocket and function to compensate for the viral replication impairment due to the primary mutation[1] or through natural polymorphisms prior to PI exposure.[13] Oftentimes, secondary polymorphisms influence inhibitor binding but crystal structures reveal that these amino acid changes are typically located in regions that do not make physical contact with the PIs.[4, 13-15] The mechanisms by which distal mutations transmit their effects to the active site pocket and confer drug resistance are unclear, but they have been implicated in altering protein flexibility[16] through the hydrophobic sliding mechanism,[17] or in restoring protein stability.[18] Recently, the transition states of native and drug-resistant HIV-1 PR were shown to be the same.[19] Because both primary and secondary mutations are present in multidrug-resistant HIV-1 PR constructs that we previously analyzed by double electron-electron resonance (DEER) spectroscopy,[20, 21] where flap conformation and flexibility are altered, we hypothesize that these mutations individually and in combinations can modify HIV-1 PR flap conformational sampling.

Site-directed spin labeling (SDSL) DEER spectroscopy (also called pulsed electron double resonance, PELDOR) is a pulsed electron paramagnetic resonance (EPR) technique that measures the strength of the dipole interaction between unpaired electrons.[22-24] This method has been applied extensively in distance measurements to study conformational changes in biomolecules.[25-30] We, and others, have previously utilized SDSL-DEER to monitor flap conformational sampling in HIV-1 PR.[20, 21, 30-35] Because HIV-1 PR is a homodimer, labeling a single amino acid residue in the polypeptide incorporates two spin labels into the

holoenzyme. Specifically, a site-specific cysteine residue is incorporated into the aqueous solvent-exposed flap sites (e.g., K55C and K55C′) for chemical modification with an EPR-active spin probe[30] (Figure 1B), where inter-spin distance in the 20–60 Å range can readily be studied by DEER.[22, 36] Previous DEER studies on HIV-1 PR have shown sampling of flap conformers consistent with conformational ensembles described as closed (or closed-like), semi-open, curled/tucked, and wide-open,[20, 21, 31, 32] where as discussed within, the curled/tucked and wide-open conformations are considered to be "open-like" states. Both X-ray diffraction and molecular dynamics (MD) simulation models[37-42] were used when assigning the conformational populations observed in our DEER distance profiles.

For PI-naïve protein sequences (*i.e.*, from patients infected with HIV-1 that have not taken any PI therapy), MD simulations show a predominant semi-open flap conformation for the apo HIV-1 PR, with only a small percentage of the conformers found in either closed-like or wide-open state.[37, 42, 43] Ligand-bound protein is shown to adopt the closed conformation, consistent with enzyme-inhibitor crystal complexes.[4, 44-46] Additional MD studies of apo protein reveal a curled/tucked conformation of the flaps, which is proposed to be a conformational trigger for flap opening.[41, 43] X-ray structures have also revealed curled flap conformations.[40] In these conformations, the flap tips curl in towards the active site, and depending on the study may or may not limit substrate and inhibitor access to the binding pocket, revealing a high degree of variability in this conformation. Based upon these studies and our analysis presented here, we hypothesize that the curled/tucked state we detect in DEER distance profiles of HIV-1 PR is a state whereby inhibitor can escape from the pocket; making it an "open" state. "Open-like" states are defined as conformers where inhibitors are likely able to escape from the binding cleft. Thus, we refer to both the wide-open and curled/tucked conformers collectively as "open-like" states.

Both DEER studies and MD simulations of two drug-resistant variants, MDR769 and V6 HIV-1 PR, have shown that the conformational sampling and average structure of the flaps are altered compared to the native protease.[20] Additional experiments have reported HIV-1 PR conformational sampling shifts attributed to subtype polymorphisms.[21] In this study, we investigate effects of individual amino acid substitutions and specific combinations of amino acid changes, as well as addition of inhibitor or substrate-mimic, on flap conformation and flexibility. In particular, SDSL-DEER was used to understand the effects of the accumulation of primary, D30N, and secondary mutations M36I and A71V on the flap conformational sampling of WT subtype B HIV-1 PR. D30N occurs specifically in response to nelfinavir treatment,[1, 3] whereas M36I and A71V, along with other non-active site substitutions, appear as a result of selective pressure of treatments using various protease inhibitors.[1, 3, 11] The locations of these sites in HIV-1 PR are shown in Figure 1A.

The effects that these combined mutations have upon the enzymatic parameters (k_{cat}, K_m, k_{cat}/K_m) was investigated previously[13] and serve as the basis for our correlation studies. DEER data analyses show that secondary mutations alter the fractional occupancy of HIV-1 PR conformational sampling profiles. By comparing the fractional occupancy of various conformational states with enzyme kinetic parameters and inhibition constants, we find that drug resistance correlates to effects of mutations such that they combine to stabilize the open-like states at the expense of the closed state. These findings also suggest that a predominantly large occupancy of the semi-open state is a likely, but maybe not sufficient,[34] requirement for catalytic efficiency. This work shows a direct link between equilibrium conformational sampling and enzyme kinetic/inhibition parameters in HIV-1 PR, and forms the basis of a hypothesis for a possible mechanism of how secondary mutations combine to elicit drug resistance. Namely, mutations combine to shift the fractional occupancy of the conformational sampling ensemble whereby the "open-like" states are stabilized at the

expense of the closed-state, while retaining a sufficiently high population of the semi-open conformation for the enzyme to maintain viral fitness.

EXPERIMENTAL PROCEDURES

Materials

The spin label, (1-oxyl-2,2,5,5-tetramethyl-Δ3-pyrroline-3-methyl) methanethiosulfonate (MTSL) was purchased from Toronto Research Chemicals (North York, ON, Canada). The QuikChange site-directed Mutagenesis Kit was acquired from Stratagene (La Jolla, CA). The pET23a vector was bought from Novagen (Gibbstown, NJ). The subtype B HIV-1 PR DNA is purchased from DNA2.0 (Menlo Park, CA). Deuterated materials, such as D_2O, D_3-NaOAc and D_8-glycerol were bought from Cambridge Isotope Laboratories (Andover, MA). Ritonavir was obtained through the AIDS Research and Reference Reagent Program. The non-hydrolyzable substrate mimic, CA-p2 (H-Arg-Val-Leu-r-Phe-Glu-Ala-Nle-NH_2, r=reduced) was acquired from the University of Florida Protein Chemistry Core Facility. Unless otherwise indicated, all reagents were purchased from Fisher Scientific (Pittsburg, PA) and used as received.

Cloning and Site-directed Mutagenesis

DNA that encodes *E. coli* codon-optimized subtype B HIV-1 PR (DNA 2.0) was cloned into pET-23a vector (Novagen) under the control of a T7 promoter. Seven stabilized (Q7K, L33I, L63I) and inactive (D25N) constructs (B_{si}) with engineered labeling sites (K55C) were made using the QuikChange site-directed mutagenesis kit by Stratagene: D30N, M36I, A71V, D30N/M36I, D30N/A71V, M36I/A71V, and D30N/M36I/A71V. Note that this procedure renders all mutations symmetrically applied to both subunits of the homodimer. Moreover, natural cysteine residues (C67 and C95) in these constructs are mutated to alanine to prevent non-specific disulfide bridge formation and to ensure site-specific labeling at C55. The C67A and C95A mutations have been utilized in numerous X-ray crystallography studies and do not alter kinetic parameters, protein stability or dimer dissociation compared to the unmutated sequence.[47, 48] The fidelity of HIV-1 PR DNA sequences was confirmed by Sanger DNA sequencing (ICBR Genomics Facility, UF).

Protein Expression, Purification, and Spin Labeling

Protein expression, purification, and spin-labeling were carried out as previously described[20] with the following modification: the inclusion bodies resuspension buffer pH used for anion exchange depends upon the isoelectric point (pI) of a given construct. The buffer pH used for wild-type (WT) subtype B (B_{si}), D30N, M36I, A71V, D30N/M36I, D30N/A71V, M36I/A71V, and D30N/M36I/A71V, respectively are as follows: 8.85, 9.00, 8.82, 8.80, 8.95, 8.98, 8.85, and 8.88. Methanethiosulfonate (MTSL) spin-label (Toronto Research Chemicals) was added in three to four-fold molar excess to 8 μM HIV-1 PR homodimer in 10 mM Tris-HCl, pH 6.9, and the reaction is allowed to proceed in the dark for 12 hours at 25 °C, 150 rpm. Homogeneous spin-labeling was verified via electrospray ionization time-of-flight mass spectrometry (ESI-TOF-MS), as shown in the Supporting Information.

Sample Preparation and DEER Data Acquisition

Protein samples were prepared as 100 μM HIV-1 PR homodimer in 20 mM D_3-NaOAc/D_2O, pH 5.0, 30% D_8-glycerol (Cambridge Isotope Laboratories). For substrate or inhibitor-bound samples, 4:1 molar excess of substrate or inhibitor was added and the sample was allowed to sit for at least 30 minutes to ensure sufficient time for binding. Samples were transferred to a 4-mm quartz EPR tube and were flash frozen in liquid nitrogen before insertion into the resonator, nominally at 65 K. All pulsed EPR data were collected in a

Bruker EleXsys E580 spectrometer equipped with the ER 4118X-MD-5 dielectric ring resonator at 65 K using a four-pulse DEER sequence,[36] described in detail previously.[20]

DEER Data Processing

The DEER dipolar modulation curves were background subtracted, long-pass filtered, and converted to distance distribution profiles via Tikhonov regularization (TKR) using DeerAnalysis2008,[49, 50] a free software from the Swiss Federal Institute of Technology Zurich website (http://www.epr.ethz.ch/software/index). Background subtraction level was determined using a self-consistent analysis procedure.[32] The optimal regularization parameter was used for the conversion of the dipolar modulation curve to a TKR distance profile. Zero time was determined by fitting the -300 to 300 ns region of the dipolar modulation curve with a Gaussian function, where the center of the Gaussian fit is equal to the zero time. Details on background subtraction, zero time calculation, optimal regularization parameter selection and the corresponding error analyses are provided in the Supporting Information.

A series of Gaussian-shaped populations representing the nominal conformations of HIV-1 PR[21, 32] with estimated relative percentage, full width at half maximum (FWHM), and most probable distance were summed to reconstruct the distance profile via DeerSim. Using this software, the dipolar evolution curve was regenerated from the summed Gaussian profile for comparison to the experimental background-subtracted data and TKR fit. DeerSim is a MatLab-based software created by our laboratory and is available upon request. χ^2 error analysis[51, 52] was performed for populations < 20% by sequentially suppressing these populations and their linear combinations. The regenerated echo curve after population suppression was compared to the TKR fit, and the χ^2 value was calculated. When χ^2 was less than the critical value at P=0.05 ($\chi^2_{0.95}$) for certain degrees of freedom (df), the questionable populations were discarded (see Supporting Information).

Pearson Criteria and Error Analysis

Pearson correlation coefficient calculation and the criteria for its interpretation have been previously established.[53] The following criterion was used: 0.8 – 1.0, strong; 0.5 – 0.8, moderate; 0.2 – 0.5, weak; 0.0 – 0.2, no association. The same criterion held true for negative correlations. Meanwhile, errors associated with percent relative populations were determined using χ^2 error analysis.[51, 52]

RESULTS

Effect of mutations on conformational sampling

The effects that accumulated primary and secondary mutations have on flap conformational sampling were determined from a series of single, double and triple mutant constructs containing amino acid substitutions D30N, M36I and A71V (all sequence details given in Supporting Information). Distance profiles between the two spin probes incorporated into the flaps at site K55C/K55C′ were determined from DEER spectroscopy (also referred to as PELDOR). Figure 2A shows time-domain, background-subtracted dipolar modulation curves for HIV-1 PR constructs studied here. Note, wild-type (WT) HIV-1 PR is referred to in our previous publications as subtype B, PMPR, or B_{si}.[20, 21, 32, 33, 52] The rate of decay and frequency of the oscillations of the dipolar modulation curves are directly related to the breadth and most probable distance of the distance profiles.[50, 54] The secondary mutation, A71V alone or in combination with either D30N or M36I (i.e., A71V, D30N/A71V, and M36I/A71V), results in a steeper echo decay at $\tau < 0.50$ μs (solid line), indicating that shorter distances consistent with a closed conformation, as seen previously upon inhibitor binding,[32, 33, 52, 55] dominate in the corresponding distance profiles. For the other constructs

investigated, the slope of the initial echo decay is similar to WT, signifying most probable distances consistent with a predominant semi-open conformation or comparable closed and semi-open populations (e.g., D30N/M36I) as seen for other apo HIV-1 PR constructs.[21, 33]

Figure 2B shows the distance profiles obtained from Tikhonov regularization (TKR) of the background-subtracted time domain dipolar modulation echo curves. For WT, D30N, M36I and D30N/M36I/A71V, the most-probable inter-spin distance occurs near 35–37 Å (dashed line), corresponding to occupancy of the semi-open conformation. For A71V, D30N/M36I, D30N/A71V, and M36I/A71V the most probable distance occurs at a shorter distance of ~ 33 Å (solid line); which is a distance consistent with a closed-like or closed conformation. Previously, this distance was only observed in DEER measurements when inhibitor was added.[31, 32] Hence, here, we distinguish between the "closed conformation" defined as a ligand-bound state and a "closed-like conformation" defined as a conformer that resembles the distance of the ligand-bound closed state but is populated in the apoenzyme. Additionally, these constructs show a marked increase in the fractional occupancy of a distance range of 26–31 Å. We hypothesize that this distance is consistent with a curled/tucked (ct) conformation of the flaps[41, 43] where the β-hairpin would be arranged in a manner that the spin labels would point towards one another, leading to a shorter distance between the spin-probes, but where the backbone conformation may produce an opening to the active site pocket allowing for inhibitor to escape. For A71V, D30N/M36I, M36I/A71V and D30N/M36I/A71V, a small but distinct peak in the distance range of 40–45 Å is observed. This distance is assigned to a wide-open (wo) flap conformation.[42, 43, 56, 57]

In a self-consistent analytical technique for background subtraction of the dipolar modulated echo curves, a series of Gaussian-shaped populations is used to regenerate the TKR distance profile and fit to the time-domain data.[21, 32] For this data analysis we assume that the ensemble of protein/spin-label conformers can be modeled by a Gaussian-shaped function. An example of the Gaussian reconstruction of the distance profile for M36I/A71V is shown in Figure 3A. The complete details for the population analyses are given in the Supporting Information. By combining model structures obtained from MD simulations and X-ray models, we assign the predominant Gaussian distance populations to four distinct ensembles of HIV-1 PR conformers.[38-45] Gaussian populations with average distances in the range of 26–31 Å are defined as curled/tucked ensembles. Meanwhile, populations centered near 33 Å are defined as closed-like conformations, whereas those near 35–37 Å are referred to as semi-open conformations. Finally, distances within 40–45 Å are described as wide-open populations. The bar graph in Figure 3B summarizes the results from the Gaussian reconstruction analyses.

Inhibitor-induced conformational sampling shift

To monitor the effect of inhibitor-binding to the flap conformational sampling of HIV-1 PR containing single point mutations, four-fold molar excess of inhibitor or substrate mimic was added to MTSL-labeled D30N, M36I, A71V and D30N/M36I/A71V subtype B HIV-1 PR constructs. The area-normalized distance profiles in the presence of the non-hydrolyzable substrate mimic (CA-p2) and ritonavir (RTV) overlaid with the apoenzyme (apo) reveal a shift of the most probable distance from 35–37 Å to 33 Å in D30N and M36I constructs (Figures 4A and B), indicating a conformational shift in favor of the closed state. The bar graphs in the figure insets show 60% and 66% increase of the closed population percentage for CA-p2 or RTV-bound D30N and M36I, respectively. The distance distribution widths narrowed substantially upon adding a substrate-mimic or inhibitor.

In contrast, the most probable distance for the A71V DEER distance profile (Figure 4C) remains unchanged at 33 Å upon addition of substrate mimic or inhibitor, suggesting that the most probable distance of 33 Å for the apoenzyme is consistent with a high occupancy of a

closed-like conformer in the absence of a ligand. Noticeably, the distance distribution widths are narrower for A71V in the presence of substrate mimic or inhibitor, with a 33% and 27% increase in the percentage occupancy of the closed state for CA-p2 and RTV, respectively. For the triple mutation construct, D30N/M36I/A71V, upon addition of CA-p2, a shift of the most probable distance occurred from 35 Å to 33 Å, similar to those observed for D30N and M36I constructs bound to CA-p2. However, in this case, addition of RTV did not induce flap closure in D30N/M36I/A71V (Figure 4D) and the most probable distance was seen to remain at 35 Å. This result is not surprising as the triple mutant shows cross resistance to various inhibitors, including RTV, and our previous DEER investigations show trends or correlations between the relative shift to the closed state, and changes in K_i [55] and IC_{50} values.[52] Note that the relative populations of the curled/tucked and wide-open conformers decreased or disappeared upon binding of CA-p2 or RTV to the triple mutant construct, suggesting that these peaks are not artifacts of analysis or misfolded/non-functional protein in our samples.

DISCUSSION

Effects of mutations to percentage occupancies of flap conformational populations

Several conclusions regarding the effects of sequential mutations on the fractional occupancy of the HIV-1 PR equilibrium conformational ensemble can be made. When compared to WT, incorporation of the D30N primary mutation does not significantly alter the conformational sampling profile, where roughly 65–70% of the conformers populate a semi-open state (Figure 3B). Strikingly, on the other hand, when either A71V or M36I is combined with D30N, a closed-like conformer dominates the ensemble, with less than 35% occupancy of the semi-open conformation. Additionally, the closed-like conformation dominates with A71V alone or in combination with M36I.

Previous X-ray crystal structure and MD investigations of the A71V polymorphism[58] show that this substitution requires a local structural adjustment in the cantilever region, particularly amino acid residues 67–71, to accommodate the bulkier valine side-chain.[58] Because the loop formed by residues 68–71 is highly mobile during flap opening and closing upon substrate/inhibitor binding,[16] it is not surprising that this single mutation can markedly shift the flap conformational sampling profile. Recent MD simulations also indicate that A71V may stabilize the dimeric form of the enzyme, which could be essential to offset effects of other mutations that alter β-hairpin conformation and destabilize the dimer interface.[59] Additional experimental studies of others have also upheld the insights from MD simulations, showing an increase in protein stability after combining A71V to a primary mutation.[18] Perhaps the thermodynamic stabilizing effects of A71V come about by a structural shift to a closed-like state as the predominant conformer of the equilibrium ensemble.

The M36 substitution with isoleucine is the most common mutation seen in the hydrophobic core of HIV-1 PR,[60] and is proposed to alter flap conformation via the hydrophobic sliding mechanism.[17] Additionally, MD simulations have shown that M36I decreases the binding cavity volume.[61] However, we find herein that the M36I mutation alone has only a minimal effect on the conformational sampling ensemble compared to native enzyme. The population of the semi-open ensemble slightly decreases with an increase of the closed and curled conformations. The small increases in these two conformations may uphold insights from MD simulations, which suggest that the decrease in the binding cavity volume results from the increase of closed-like population.

When M36I and A71V secondary polymorphisms are combined with primary mutation D30N, the fractional occupancy resembles that of native enzyme in that the semi-open state

now becomes the most predominant conformation in the ensemble. However, in contrast to native enzyme, the conformational sampling profile of the triple mutation construct shows a synchronized increase in the percentage of the wide-open and curled conformations with a decrease in the closed population percentage. The D30N/M36I/A71V construct has been reported to have weaker inhibition (higher K_i) for nelfinavir, indinavir, and ritonavir, and better catalytic efficiency with respect to WT.[13] The recovery of a major semi-open population via accumulation of primary and secondary mutations suggests a mechanism by which mutations combine in HIV-1 PR to recover catalytic efficiency while eluding inhibitors.

Correlation of DEER conformational sampling with enzyme kinetics and inhibition parameters

Statistical correlations, via Pearson product moment correlation,[62] were made between the fractional occupancies of conformational states determined from DEER distance profiles, and published kinetics and inhibition data. Note that our EPR constructs differ from those used in enzymatic investigations (sequences given in Supporting Information). DEER samples contain the K55R1 spin-label site and the catalytic residue substitution D25N. This substitution is often used in spectroscopic studies[63-68] because of the relative ease of sample preparation, and sample stability and homogeneity. The D25N mutation has been shown to not significantly change the protein structure, although, it does increase inhibitor dissociation (K_d)[63] by up to a factor of ~10^6. The experimental ease of using the D25N constructs has been validated in our earlier SDSL EPR investigations showing correlations among inhibitor-induced flap closure with NMR investigated ligand-exchange dynamics and with IC_{50} values for a multidrug resistant HIV-1 PR construct.[52, 55] Although NMR investigations reveal differences in D25 versus D25N dynamics and monomer/dimer dissociation constants,[63] our data for the D25N constructs do show strong correlations among DEER distance profiles and in vitro kinetic/inhibition data. Slight differences in our results may be anticipated for the active D25 construct, but due to autodegradation, our DEER signal intensities from apo active enzymes are too weak for the data analysis required within.

Pearson product moment correlation coefficient values (r) of -0.84, -0.73, and -0.19 were obtained for the fractional occupancy; *i.e*., the relative percentage, of the closed conformation (%C) with k_{cat}, k_{cat}/K_m, and K_m;[13] respectively (correlation plots in Supporting Information). Note that when the magnitude of the Pearson's r is > 0.80, the correlation is considered significant; *i.e*., "strong," because the two-tailed critical value for r at $P = 0.05$ for a sample size of 8 is 0.707.[69] As shown in Figure 5A, a "strong" inverse trend (r = -0.84) is obtained between %C and reported values for k_{cat}[13] meaning, a higher percentage closed-like population coincides with lower catalytic rate. This finding appears reasonable given that substrate entry requires flap opening, and mutations that stabilize a closed-like conformation could have reduced turnover rates. NMR studies of substrate binding in HIV-1 PR suggest that in order for substrate uptake to occur, the flaps would have to open first, followed by slow flap closure and concomitant positioning of the substrate into a reactive geometry in the binding cleft.[67] Thus, if HIV-1 PR is initially in the closed-like state, the protease would need to adopt an open conformation for substrate entry; then a rate-limiting flap closure and concurrent positioning of substrate in the active site would ensue prior to catalysis, which can explain the observed correlation between the lowered catalytic rate in constructs that have high closed-like population. Meanwhile, we find little to no correlation with K_m (r = -0.19), thus explaining the slightly weaker correlation (r = -0.73) seen between %C and k_{cat}/K_m. The lack of correlation between %C and K_m is not surprising given only D30N occurs within the active site pocket and crystal

structures show that the incorporation of A71V along with D30N does not alter the shape of the substrate binding pocket (Supporting Information).[58]

Stronger correlation are observed when values of inhibition constants (K_i)[13] for inhibitors were plotted against the ratio of the closed-like conformation to the open-like states, as demonstrated in Figure 5B for the inhibitor, ritonavir. The rationale for combining the population of the wide-open conformers (distance ~43 Å) with the curled/tucked conformers (distances ~25–30 Å) comes from the mathematical model that best correlates our data. When only single populations were considered as the models for obtaining correlations, lower correlation coefficients (r) were obtained (Table 1). Hence, the model that best fit correlations among the data combine these two states and suggests that the curled/tucked population seen in our DEER distance profiles may correspond to a state where inhibitor can easily escape. In fact, Table 1 shows strong Pearson correlation coefficients of -0.98, -0.91 and -0.95 were calculated for this model of combining the open-like populations in the ratio of %closed-like/open-like and K_i when all three inhibitors; nelfinavir (NFV), ritonavir (RTV), and indinavir (IDV); were examined (correlation plots in Supporting Information). These findings suggest an interpretation of how cross resistance is elicited by the combination of primary and secondary mutations; specifically, that an increase in the population of “open-like” states, where inhibitor can escape, with a concomitant decrease in the population of the closed state, where inhibitor binding is stabilized, leads to larger values of inhibition constants, indicating weaker inhibitor binding strengths and thus, resistance.

Furthermore, these correlations show that enzymatic activity is compromised when the combination of mutations increase the fractional occupancy of the closed-like conformation relative to WT subtype B protease. The correlations between inhibitor binding and conformational sampling also show that alternative flap opening modes that could promote weaker inhibitor interactions, like the curled and tucked states, need to be considered when discussing drug resistance mechanisms. This point was recently demonstrated via X-ray crystallography of an extremely drug-resistant variant found in an open-like conformation.[70] Therefore, drug resistance appears when co-evolving mutations destabilize the closed state in favor of open-like conformations to elude inhibitor binding, while maintaining a semi-open population similar to wild-type so as to sustain catalytic efficiency.

Inhibitor-induced flap closure and drug resistance

The ligand-bound DEER distance profiles in Figure 4 suggest that both the substrate mimic, CA-p2 and ritonavir could efficiently induce a shift in the conformational ensemble to the closed state of D30N, M36I and A71V single point mutation constructs. Unlike D30N and M36I, the A71V construct has a predominant closed-like population in the apo state. The same flap distance of ~33 Å observed for the closed-like state in the apoenzyme and the closed conformation upon inhibitor binding suggests that these states are indistinguishable and validates that the incorporation of a single point A71V mutation results in promoting the closed flap conformation. Moreover, open-like states (i.e., curled/tucked and wide-open populations) almost disappeared completely after adding a ligand to all single-point mutation constructs (≤5%), suggesting that inhibitor or substrate-binding imposes a steric strain onto the flaps, making open-like conformations less probable. Also note that the distance distribution widths were narrower after ligand-binding, as previously observed,[32, 52] implying that binding to the substrate-mimic or inhibitor confers conformational rigidity as the flaps are locked-in onto the ligand in the binding cleft. Interestingly, for the triple mutation construct, D30N/M36I/A71V, the substrate mimic CA-p2 induced flap closure, but not RTV. Since this construct is known to be resistant to RTV based on K_i measurements,[13] it is not surprising that flap closure was not observed after adding this inhibitor. Although flap closure was not observed, presence of the ligand

prevented the flaps to adopt open-like conformational states, and promote the semi-open conformation, suggesting that the inhibitor may be loosely bound within the pocket but not interacting strongly enough for a fully closed conformation to be seen in the DEER distance profile. This finding is consistent with results seen for a multidrug resistant variant MDR769 [52] that showed disappearance of the wide-open population and displayed no substantial flap closure after adding RTV.

Hypothetical thermodynamic profiles

We hypothesize that the distance population near 26–31 Å, a distance range seen in almost all DEER distance profiles of single point mutant constructs, drug resistance constructs and various subtypes or circulating recombinant forms investigated by our lab to date,[20, 21, 32, 33, 52, 55] to be representative of a conformational ensemble where the flaps adopt a curled/tucked geometry. Inhibitor-bound DEER data reveals that the addition of CA-p2 or RTV results in the simultaneous disappearance of the wide-open and curled/tucked populations, suggesting that these distances correspond to "real" conformational states of HIV-1 PR and do not necessarily represent signals from misfolded or non-functional protein contaminants in our samples. We hypothesize that this conformational state may represent an alternative flap opening mechanism, suggested previously by others,[41, 43] where the β-hairpin would be arranged in a manner that the spin labels would point towards one another, leading to a shorter distance between the spin-probes, but where the backbone conformation may produce an opening to the active site pocket allowing for inhibitor to escape.

Figures 6A and 6B provide a graphical interpretation of the results of our population analyses for WT subtype B and D30N/M36I/A71V constructs; respectively, in terms of hypothetical thermodynamic profiles. In these figures, the relative energy of the semi-open states is aligned. The probability distribution profiles are directly converted to the thermodynamic energies via the relationship $\Delta G = -RT \ln P_i$, where T was taken as 300 K (because we assume that freezing traps the equilibrium conformational sampling at room temperature prior to freezing)[71] and P_i determined from the normalized population probability. Because we are suggesting that the curled/tucked state is an alternate conformer where inhibitor can escape,[41] the curled/tucked and wide-open ensembles are combined into the single open-like state for these energy landscapes. Note that in these thermodynamic profiles, the heights of the barriers between the states are unknown from DEER investigations. Only the relative free energies of the states can be obtained from the population analyses. Compared to the WT construct, the combined mutations act to stabilize the free energy of the open-like conformations while concurrently destabilize the free energy of the closed-like conformation relative to the free energy of the semi-open state. This effect can be seen clearly in Figure 7, where the relative percentage change of the population of each conformation for each variant is compared to WT. It is clear that most of the variants have a destabilized semi-open conformation, but have increased curled/tucked and closed-like populations. The triple mutant, however, has a destabilized closed state, a semi-open population similar to WT, and increased populations of both the curled/tucked and wide-open conformational states.

CONCLUSIONS

Using DEER, we have shown that both primary and secondary mutations alter conformational sampling in HIV-1 PR. The secondary mutation A71V promotes a closed-like conformation of the protease except when both D30N and M36I mutations are present. The recovery of a predominant semi-open population in D30N/M36I/A71V after the step-wise incorporation of these mutations suggests the importance of the semi-open conformation in maintaining turnover rate and catalytic efficiency. On the other hand, the

"strong" inverse Pearson correlation for the percentage of closed conformation vs. k_{cat} implies that certain mutations that promote the closed-like conformation (i.e., A71V) could hamper substrate entry resulting in lowered catalytic rate. However, a more closed-like conformation may also stabilize protease-inhibitor interactions, as demonstrated by "strong" correlations among the ratio of closed-like to open-like population percentages with K_i values for NFV, RTV, and IDV. This result implies that drug resistance emerges when the mutations combine to increase the population of "open-like" states at the expense of the closed-like conformation, while maintaining a semi-open population similar to WT. This is corroborated by the lack of flap closure upon adding RTV to D30N/M36I/A71V, a construct that exhibited resistance to this inhibitor based on K_i measurements. We have previously demonstrated using a multi-drug resistant HIV protease variant MDR769 that the lack of inhibitor-induced flap closure is correlated to drug resistance based on IC_{50} measurements.[52] These correlation measurements with k_{cat} and K_i show that by accumulating mutations, HIV-1 PR could recover close to WT catalytic efficiency while eluding inhibitors.

These results indicate a possible mechanism for drug resistance where the population of a thermodynamic state is altered. Alternative hypotheses for how drug resistance is affected in HIV-1 PR also evoke the idea that protein dynamics, hydrophobic core flexibility[72] or the exchange rates among conformational states[73] are altered by secondary mutations, which in turn modulates enzyme function. In fact, numerous MD simulations provide insights into hypotheses where protein backbone dynamics and flexibility are altered.[72-74]

From an experimental approach, NMR investigations of protein conformational exchange and dynamics have a strong hold.[75, 76] Although the backbone dynamics of the native subtype B construct have been explored extensively,[64, 65, 67, 68,77] the exchange rates in native HIV-1 PR are difficult to characterize due to the fast dynamics of the flaps and relatively slower time scale of the exchange process.[74] Recently, exchange dynamics were measured on a synthetic tethered HIV-1 PR construct revealing that mutations may alter the rate of exchange among the states, thus impacting catalysis.[34] It is likely that a combination of effects is at play to generate drug resistance, and possibly, a combination of all these aspects of the protein are changing as drug pressure selected mutations arise.

Supplementary Material

Refer to Web version on PubMed Central for supplementary material.

Acknowledgments

We would like to thank Dr. Steve Hagen for access to his circular dichroism spectrometer, Dr. Alexander Angerhofer for his help in maintaining the Bruker E580 EPR spectrometer and Dr. Adrian Roitberg for the helpful conversations.

Funding

This work was supported by NSF MBC-0746533 (GEF), NIH R37 AI28571 (BMD), UF Center for AIDS Research, and NHMFL-IHRP.

References

1. Weber IT, Agniswamy J. HIV-1 Protease: Structural Perspectives on Drug Resistance. Viruses. 2009; 1:1110–1136. [PubMed: 21994585]
2. Anderson AC. Winning the arms race by improving drug discovery against mutating targets. ACS Chem Biol. 2012; 7:278–288. [PubMed: 22050347]

3. Kantor R, Fessel WJ, Zolopa AR, Israelski D, Shulman N, Montoya JG, Harbour M, Schapiro JM, Shafer RW. Evolution of primary protease inhibitor resistance mutations during protease inhibitor salvage therapy. Antimicrob Agents Chemother. 2002; 46:1086–1092. [PubMed: 11897594]
4. Mahalingam B, Boross P, Wang YF, Louis JM, Fischer CC, Tozser J, Harrison RW, Weber IT. Combining mutations in HIV-1 protease to understand mechanisms of resistance. Proteins. 2002; 48:107–116. [PubMed: 12012342]
5. Csermely P, Palotai R, Nussinov R. Induced fit, conformational selection and independent dynamic segments: an extended view of binding events. Trends Biochem Sci. 2010; 35:539–546. [PubMed: 20541943]
6. Ma B, Nussinov R. Enzyme dynamics point to stepwise conformational selection in catalysis. Curr Opin Chem Biol. 2010; 14:652–659. [PubMed: 20822947]
7. Miller Y, Ma B, Nussinov R. Polymorphism in Alzheimer Abeta amyloid organization reflects conformational selection in a rugged energy landscape. Chem Rev. 2010; 110:4820–4838. [PubMed: 20402519]
8. Joint United Nations Programme on HIV/AIDS (UNAIDS). UNAIDS Report on the Global AIDS Epidemic. 2010:19–57.
9. Huff JR. Hiv Protease - a Novel Chemotherapeutic Target for Aids. Journal of Medicinal Chemistry. 1991; 34:2305–2314. [PubMed: 1875332]
10. Wlodawer A, Vondrasek J. Inhibitors of HIV-1 protease: a major success of structure-assisted drug design. Annu Rev Biophys Biomol Struct. 1998; 27:249–284. [PubMed: 9646869]
11. Martinez-Cajas JL, Wainberg MA. Protease inhibitor resistance in HIV-infected patients: molecular and clinical perspectives. Antiviral Res. 2007; 76:203–221. [PubMed: 17673305]
12. Wilson SI, Phylip LH, Mills JS, Gulnik SV, Erickson JW, Dunn BM, Kay J. Escape mutants of HIV-1 proteinase: enzymic efficiency and susceptibility to inhibition. Biochim Biophys Acta. 1997; 1339:113–125. [PubMed: 9165106]
13. Clemente JC, Hemrajani R, Blum LE, Goodenow MM, Dunn BM. Secondary mutations M36I and A71V in the human immunodeficiency virus type 1 protease can provide an advantage for the emergence of the primary mutation D30N. Biochemistry. 2003; 42:15029–15035. [PubMed: 14690411]
14. Mo H, Parkin N, Stewart KD, Lu L, Dekhtyar T, Kempf DJ, Molla A. Identification and structural characterization of I84C and I84A mutations that are associated with high-level resistance to human immunodeficiency virus protease inhibitors and impair viral replication. Antimicrob Agents Chemother. 2007; 51:732–735. [PubMed: 17101675]
15. Clemente JC, Moose RE, Hemrajani R, Whitford LR, Govindasamy L, Reutzel R, McKenna R, Agbandje-McKenna M, Goodenow MM, Dunn BM. Comparing the accumulation of active- and nonactive-site mutations in the HIV-1 protease. Biochemistry. 2004; 43:12141–12151. [PubMed: 15379553]
16. Piana S, Carloni P, Rothlisberger U. Drug resistance in HIV-1 protease: Flexibility-assisted mechanism of compensatory mutations. Protein Sci. 2002; 11:2393–2402. [PubMed: 12237461]
17. Foulkes-Murzycki JE, Scott WR, Schiffer CA. Hydrophobic sliding: a possible mechanism for drug resistance in human immunodeficiency virus type 1 protease. Structure. 2007; 15:225–233. [PubMed: 17292840]
18. Chang MW, Torbett BE. Accessory mutations maintain stability in drug-resistant HIV-1 protease. J Mol Biol. 2011; 410:756–760. [PubMed: 21762813]
19. Kipp DR, Hirschi JS, Wakata A, Goldstein H, Schramm VL. Transition states of native and drug-resistant HIV-1 protease are the same. Proc Natl Acad Sci U S A. 2012; 109:6543–6548. [PubMed: 22493227]
20. Galiano L, Ding F, Veloro AM, Blackburn ME, Simmerling C, Fanucci GE. Drug pressure selected mutations in HIV-1 protease alter flap conformations. J Am Chem Soc. 2009; 131:430–431. [PubMed: 19140783]
21. Kear JL, Blackburn ME, Veloro AM, Dunn BM, Fanucci GE. Subtype polymorphisms among HIV-1 protease variants confer altered flap conformations and flexibility. J Am Chem Soc. 2009; 131:14650–14651. [PubMed: 19788299]

22. Jeschke G. Distance measurements in the nanometer range by pulse EPR. Chemphyschem. 2002; 3:927–932. [PubMed: 12503132]
23. Jeschke G, Polyhach Y. Distance measurements on spin-labelled biomacromolecules by pulsed electron paramagnetic resonance. Phys Chem Chem Phys. 2007; 9:1895–1910. [PubMed: 17431518]
24. Pannier M, Veit S, Godt A, Jeschke G, Spiess HW. Dead-time free measurement of dipole-dipole interactions between electron spins. J Magn Reson. 2000; 142:331–340. [PubMed: 10648151]
25. Cai Q, Kusnetzow AK, Hideg K, Price EA, Haworth IS, Qin PZ. Nanometer distance measurements in RNA using site-directed spin labeling. Biophys J. 2007; 93:2110–2117. [PubMed: 17526583]
26. Finiguerra MG, Prudencio M, Ubbink M, Huber M. Accurate long-range distance measurements in a doubly spin-labeled protein by a four-pulse, double electron-electron resonance method. Magn Reson Chem. 2008; 46:1096–1101. [PubMed: 18932181]
27. Gruene T, Cho MK, Karyagina I, Kim HY, Grosse C, Giller K, Zweckstetter M, Becker S. Integrated analysis of the conformation of a protein-linked spin label by crystallography, EPR and NMR spectroscopy. J Biomol NMR. 2011; 49:111–119. [PubMed: 21271275]
28. Fleissner MR, Bridges MD, Brooks EK, Cascio D, Kalai T, Hideg K, Hubbell WL. Structure and dynamics of a conformationally constrained nitroxide side chain and applications in EPR spectroscopy. Proc Natl Acad Sci U S A. 2011; 108:16241–16246. [PubMed: 21911399]
29. Swanson MA, Kathirvelu V, Majtan T, Frerman FE, Eaton GR, Eaton SS. DEER distance measurement between a spin label and a native FAD semiquinone in electron transfer flavoprotein. J Am Chem Soc. 2009; 131:15978–15979. [PubMed: 19886689]
30. Fanucci GE, Cafiso DS. Recent advances and applications of site-directed spin labeling. Curr Opin Struct Biol. 2006; 16:644–653. [PubMed: 16949813]
31. Torbeev VY, Raghuraman H, Mandal K, Senapati S, Perozo E, Kent SB. Dynamics of “flap” structures in three HIV-1 protease/inhibitor complexes probed by total chemical synthesis and pulse-EPR spectroscopy. J Am Chem Soc. 2009; 131:884–885. [PubMed: 19117390]
32. Blackburn ME, Veloro AM, Fanucci GE. Monitoring inhibitor-induced conformational population shifts in HIV-1 protease by pulsed EPR spectroscopy. Biochemistry. 2009; 48:8765–8767. [PubMed: 19691291]
33. Galiano L, Bonora M, Fanucci GE. Inter-flap distances in HIV-1 Protease determined by pulsed EPR measurements. J Am Chem Soc. 2007; 129:11004–11005. [PubMed: 17705389]
34. Torbeev VY, Raghuraman H, Hamelberg D, Tonelli M, Westler WM, Perozo E, Kent SB. Protein conformational dynamics in the mechanism of HIV-1 protease catalysis. Proc Natl Acad Sci U S A. 2011; 108:20982–20987. [PubMed: 22158985]
35. Galiano L, Blackburn ME, Veloro AM, Bonora M, Fanucci GE. Solute effects on spin labels at an aqueous-exposed site in the flap region of HIV-1 protease. J Phys Chem B. 2009; 113:1673–1680. [PubMed: 19146430]
36. Tsvetkov YD, Grishin YA. Techniques for EPR Spectroscopy of Pulsed Electron Double Resonance (PELDOR): A Review. Instruments and Experimental Techniques. 2009; 52:615–636.
37. Ding F, Layten M, Simmerling C. Solution structure of HIV-1 protease flaps probed by comparison of molecular dynamics simulation ensembles and EPR experiments. J Am Chem Soc. 2008; 130:7184–7185. [PubMed: 18479129]
38. Spinelli S, Liu QZ, Alzari PM, Hirel PH, Poljak RJ. The three-dimensional structure of the aspartyl protease from the HIV-1 isolate BRU. Biochimie. 1991; 73:1391–1396. [PubMed: 1799632]
39. Rick SW, Erickson JW, Burt SK. Reaction path and free energy calculations of the transition between alternate conformations of HIV-1 protease. Proteins. 1998; 32:7–16. [PubMed: 9672038]
40. Heaslet H, Rosenfeld R, Giffin M, Lin YC, Tam K, Torbett BE, Elder JH, McRee DE, Stout CD. Conformational flexibility in the flap domains of ligand-free HIV protease. Acta Crystallogr D Biol Crystallogr. 2007; 63:866–875. [PubMed: 17642513]
41. Scott WR, Schiffer CA. Curling of flap tips in HIV-1 protease as a mechanism for substrate entry and tolerance of drug resistance. Structure. 2000; 8:1259–1265. [PubMed: 11188690]

42. Hornak V, Okur A, Rizzo RC, Simmerling C. HIV-1 protease flaps spontaneously open and reclose in molecular dynamics simulations. Proc Natl Acad Sci U S A. 2006; 103:915–920. [PubMed: 16418268]
43. Toth G, Borics A. Flap opening mechanism of HIV-1 protease. J Mol Graph Model. 2006; 24:465–474. [PubMed: 16188477]
44. Bandaranayake RM, Kolli M, King NM, Nalivaika EA, Heroux A, Kakizawa J, Sugiura W, Schiffer CA. The effect of clade-specific sequence polymorphisms on HIV-1 protease activity and inhibitor resistance pathways. J Virol. 84:9995–10003. [PubMed: 20660190]
45. Klei HE, Kish K, Lin PF, Guo Q, Friborg J, Rose RE, Zhang Y, Goldfarb V, Langley DR, Wittekind M, Sheriff S. X-ray crystal structures of human immunodeficiency virus type 1 protease mutants complexed with atazanavir. J Virol. 2007; 81:9525–9535. [PubMed: 17537865]
46. Shen CH, Wang YF, Kovalevsky AY, Harrison RW, Weber IT. Amprenavir complexes with HIV-1 protease and its drug-resistant mutants altering hydrophobic clusters. FEBS J. 277:3699–3714. [PubMed: 20695887]
47. Louis JM, Clore GM, Gronenborn AM. Autoprocessing of HIV-1 protease is tightly coupled to protein folding. Nat Struct Biol. 1999; 6:868–875. [PubMed: 10467100]
48. Liu F, Kovalevsky AY, Tie Y, Ghosh AK, Harrison RW, Weber IT. Effect of flap mutations on structure of HIV-1 protease and inhibition by saquinavir and darunavir. J Mol Biol. 2008; 381:102–115. [PubMed: 18597780]
49. Chiang YW, Borbat PP, Freed JH. The determination of pair distance distributions by pulsed ESR using Tikhonov regularization. J Magn Reson. 2005; 172:279–295. [PubMed: 15649755]
50. Jeschke G, Chechik V, Ionita P, Godt A, Zimmermann H, Banham J, Timmel CR, Hilger D, Jung H. DeerAnalysis2006 - a comprehensive software package for analyzing pulsed ELDOR data. Applied Magnetic Resonance. 2006; 30:473–498.
51. Gabrys CM, Yang J, Weliky DP. Analysis of local conformation of membrane-bound and polycrystalline peptides by two-dimensional slow-spinning rotor-synchronized MAS exchange spectroscopy. J Biomol NMR. 2003; 26:49–68. [PubMed: 12766402]
52. de Vera IMS, Blackburn ME, Fanucci GE. Correlating conformational shift induction with altered inhibitor potency in a multidrug resistant HIV-1 protease variant. Biochemistry. 2012; 51:7813–7815. [PubMed: 23009326]
53. Zou KH, Tuncali K, Silverman SG. Correlation and simple linear regression. Radiology. 2003; 227:617–622. [PubMed: 12773666]
54. Jeschke G, Panek G, Godt A, Bender A, Paulsen H. Data analysis procedures for pulse ELDOR measurements of broad distance distributions. Applied Magnetic Resonance. 2004; 26:223–244.
55. Huang X, de Vera IM, Veloro AM, Blackburn ME, Kear JL, Carter JD, Rocca JR, Simmerling C, Dunn BM, Fanucci GE. Inhibitor-Induced Conformational Shifts and Ligand-Exchange Dynamics for HIV-1 Protease Measured by Pulsed EPR and NMR Spectroscopy. J Phys Chem B. 2012; 116:14235–14244. [PubMed: 23167829]
56. Sadiq SK, De Fabritiis G. Explicit solvent dynamics and energetics of HIV-1 protease flap opening and closing. Proteins. 78:2873–2885. [PubMed: 20715057]
57. Tozzini V, Trylska J, Chang CE, McCammon JA. Flap opening dynamics in HIV-1 protease explored with a coarse-grained model. J Struct Biol. 2007; 157:606–615. [PubMed: 17029846]
58. Kozisek M, Bray J, Rezacova P, Saskova K, Brynda J, Pokorna J, Mammano F, Rulisek L, Konvalinka J. Molecular analysis of the HIV-1 resistance development: enzymatic activities, crystal structures, and thermodynamics of nelfinavir-resistant HIV protease mutants. J Mol Biol. 2007; 374:1005–1016. [PubMed: 17977555]
59. Wright DW, Coveney PV. Resolution of discordant HIV-1 protease resistance rankings using molecular dynamics simulations. J Chem Inf Model. 2011; 51:2636–2649. [PubMed: 21902276]
60. Rhee SY, Fessel WJ, Zolopa AR, Hurley L, Liu T, Taylor J, Nguyen DP, Slome S, Klein D, Horberg M, Flamm J, Follansbee S, Schapiro JM, Shafer RW. HIV-1 Protease and reverse-transcriptase mutations: correlations with antiretroviral therapy in subtype B isolates and implications for drug-resistance surveillance. J Infect Dis. 2005; 192:456–465. [PubMed: 15995959]

61. Ode H, Matsuyama S, Hata M, Neya S, Kakizawa J, Sugiura W, Hoshino T. Computational characterization of structural role of the non-active site mutation M36I of human immunodeficiency virus type 1 protease. J Mol Biol. 2007; 370:598–607. [PubMed: 17524421]
62. Weinberg, SL.; Abramowitz, SK., editors. Statistics using SPSS: an Integrative Approach. 2008.
63. Sayer JM, Liu F, Ishima R, Weber IT, Louis JM. Effect of the active site D25N mutation on the structure, stability, and ligand binding of the mature HIV-1 protease. J Biol Chem. 2008; 283:13459–13470. [PubMed: 18281688]
64. Ishima R, Freedberg DI, Wang YX, Louis JM, Torchia DA. Flap opening and dimer-interface flexibility in the free and inhibitor-bound HIV protease, and their implications for function. Structure. 1999; 7:1047–1055. [PubMed: 10508781]
65. Ishima R, Torchia DA. Extending the range of amide proton relaxation dispersion experiments in proteins using a constant-time relaxation-compensated CPMG approach. J Biomol NMR. 2003; 25:243–248. [PubMed: 12652136]
66. Ishima R, Torchia DA, Louis JM. Mutational and structural studies aimed at characterizing the monomer of HIV-1 protease and its precursor. J Biol Chem. 2007; 282:17190–17199. [PubMed: 17412697]
67. Katoh E, Louis JM, Yamazaki T, Gronenborn AM, Torchia DA, Ishima R. A solution NMR study of the binding kinetics and the internal dynamics of an HIV-1 protease-substrate complex. Protein Sci. 2003; 12:1376–1385. [PubMed: 12824484]
68. Louis JM, Ishima R, Torchia DA, Weber IT. HIV-1 protease: structure, dynamics, and inhibition. Adv Pharmacol. 2007; 55:261–298. [PubMed: 17586318]
69. Sheskin, DJ. Handbook of Parametric and Nonparametric Statistical Procedures. 4. Chapman and Hall/CRC; New York: 2007.
70. Agniswamy J, Shen CH, Aniana A, Sayer JM, Louis JM, Weber IT. HIV-1 Protease with 20 Mutations Exhibits Extreme Resistance to Clinical Inhibitors through Coordinated Structural Rearrangements. Biochemistry. 2012; 51:2819–2828. [PubMed: 22404139]
71. Georgieva ER, Roy AS, Grigoryants VM, Borbat PP, Earle KA, Scholes CP, Freed JH. Effect of freezing conditions on distances and their distributions derived from Double Electron Electron Resonance (DEER): a study of doubly-spin-labeled T4 lysozyme. J Magn Reson. 2012; 216:69–77. [PubMed: 22341208]
72. Mittal S, Cai Y, Nalam MN, Bolon DN, Schiffer CA. Hydrophobic core flexibility modulates enzyme activity in HIV-1 protease. J Am Chem Soc. 2012; 134:4163–4168. [PubMed: 22295904]
73. Perryman AL, Lin JH, McCammon JA. HIV-1 protease molecular dynamics of a wild-type and of the V82F/I84V mutant: possible contributions to drug resistance and a potential new target site for drugs. Protein Sci. 2004; 13:1108–1123. [PubMed: 15044738]
74. Cai Y, Yilmaz N, Myint W, Ishima R, Schiffer CA. Differential Flap Dynamics in Wild-Type and a Drug Resistant Variant of HIV-1 Protease Revealed by Molecular Dynamics and NMR Relaxation. J Chem Theory Comput. 2012; 8:3452–3462. [PubMed: 23144597]
75. Kempf JG, Loria JP. Measurement of intermediate exchange phenomena. Methods Mol Biol. 2004; 278:185–231. [PubMed: 15317998]
76. Loria JP, Berlow RB, Watt ED. Characterization of enzyme motions by solution NMR relaxation dispersion. Acc Chem Res. 2008; 41:214–221. [PubMed: 18281945]
77. Myint W, Cai Y, Schiffer CA, Ishima R. Quantitative comparison of errors in (15)N transverse relaxation rates measured using various CPMG phasing schemes. J Biomol NMR. 2012; 53:13–23. [PubMed: 22466935]

ABBREVIATIONS

HIV-1 PR	HIV-1 protease
PI	protease inhibitors
DEER	double electron-electron resonance
PELDOR	pulsed electron double resonance

SDSL	site-directed spin-labeling
TKR	Tikhonov regularization
EPR	electron paramagnetic resonance
MTSL	methanethiosulfonate
B_{si}	stabilized and inactive subtype B HIV-1 protease
WT	wild-type
RTV	ritonavir
NFV	nelfinavir
IDV	indinavir

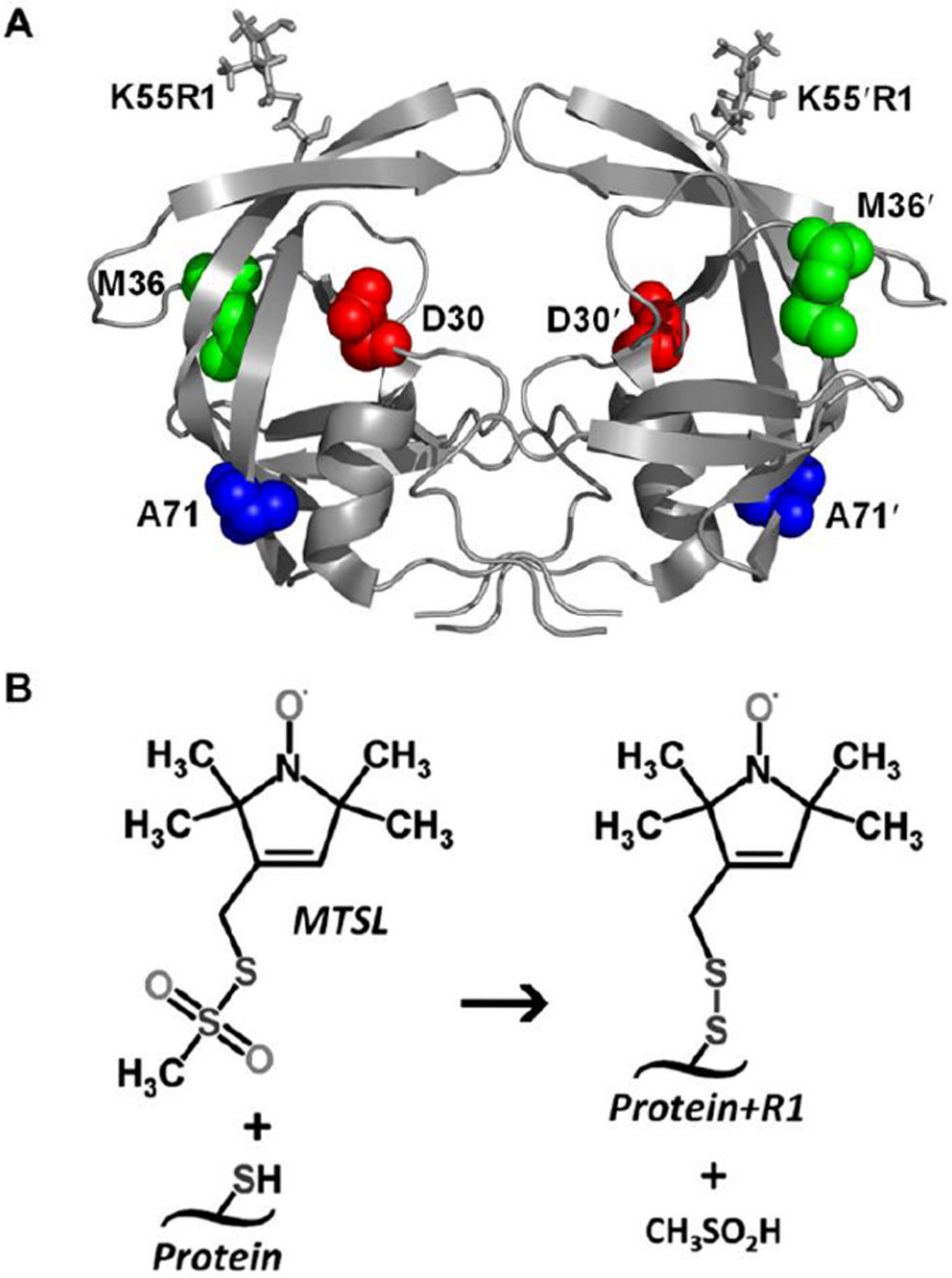

Figure 1.

(A) Ribbon diagram of HIV-1 PR (PDBID: 1HHP) rendered using PyMol modeling software. The spin probes (K55R1) are incorporated in-silico via MMM 2011.1 and shown as capped sticks. Mutation sites D30, M36 and A71 are shown as red, green and blue spheres; respectively. (B) The sulfhydryl-specific spin-labeling reaction yielding the disulfide-linked MTSL spin label at K55C, referred to as K55R1 after labeling.

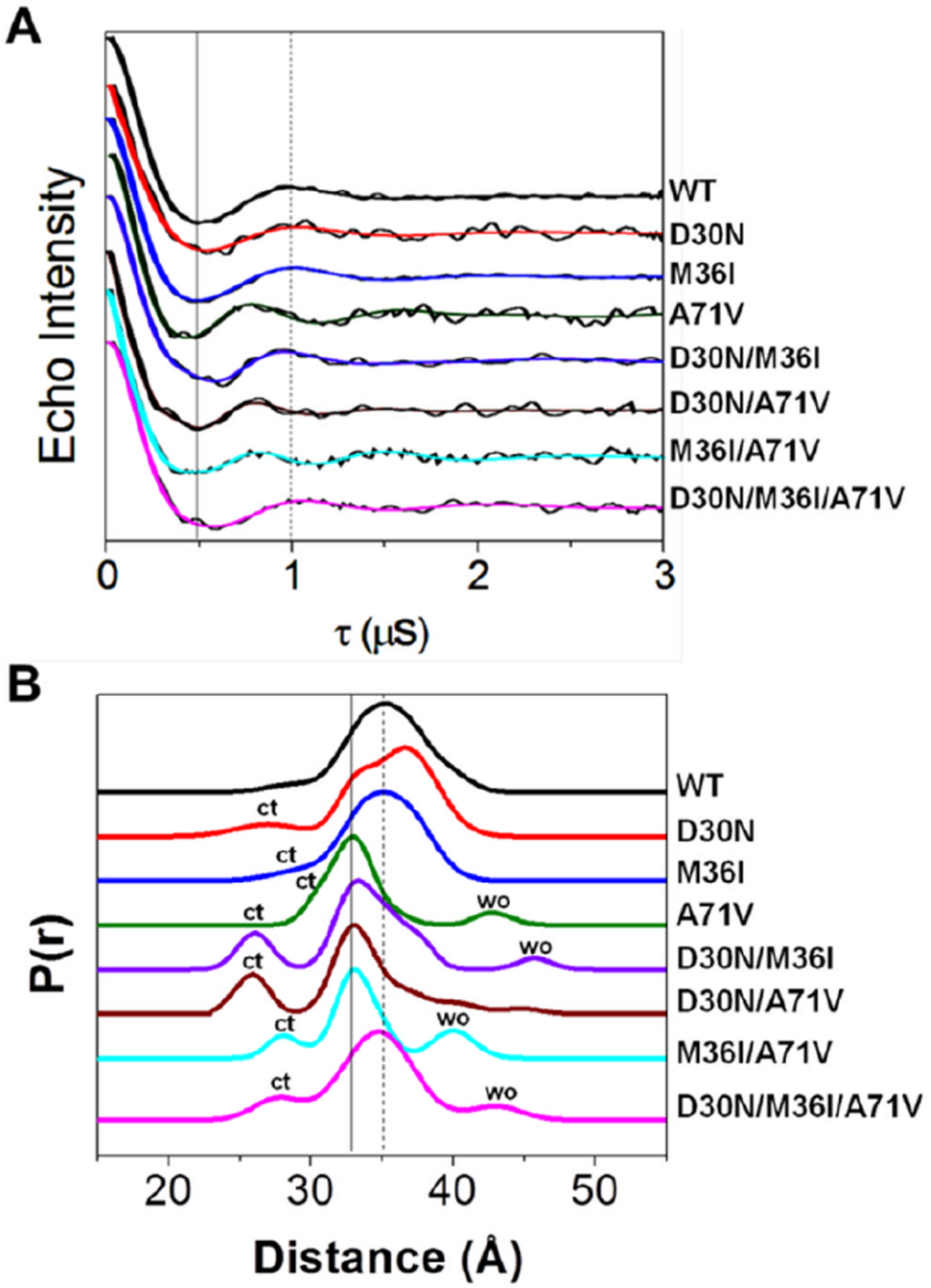

Figure 2.

(A) Background-subtracted and long-pass filtered dipolar modulation curves in the time domain for WT subtype B and for constructs with D30N, M36I, and A71V single and combined mutations overlaid with Tikhonov regularization (TKR) fits. The solid and dashed vertical lines mark the local minimum and maximum of the WT echo curve, respectively. (B) Stack plot of the corresponding TKR distance profiles. The dashed line corresponds to the semi-open conformation and the solid line indicates the peak position of the closed state. Peaks marked with ct indicate an increase in the curled/tucked population while those marked with wo signify an increase in the wide-open population.

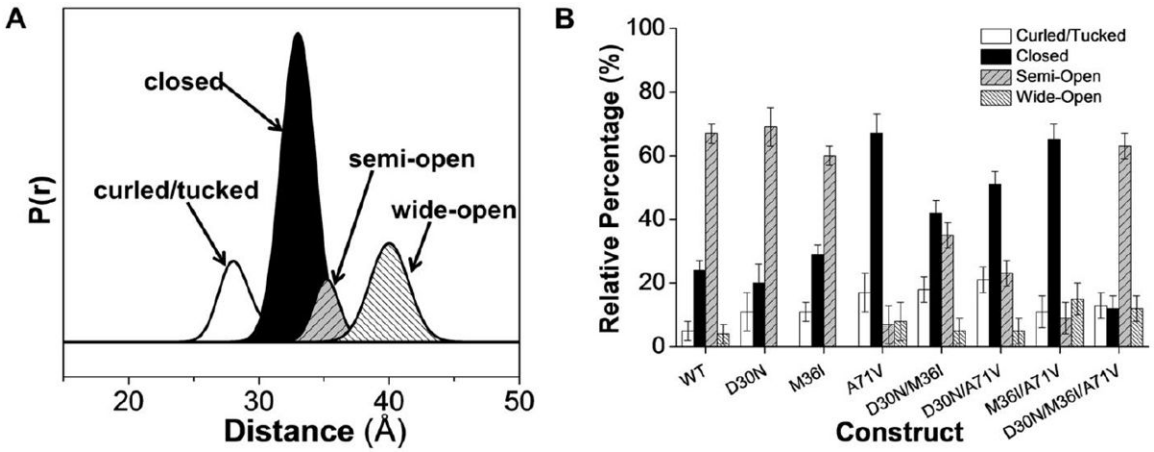

Figure 3.

(A) Gaussian reconstruction profile for M36I/A71V. (B) Results from Gaussian reconstruction analysis of the TKR distance profiles for the various constructs.

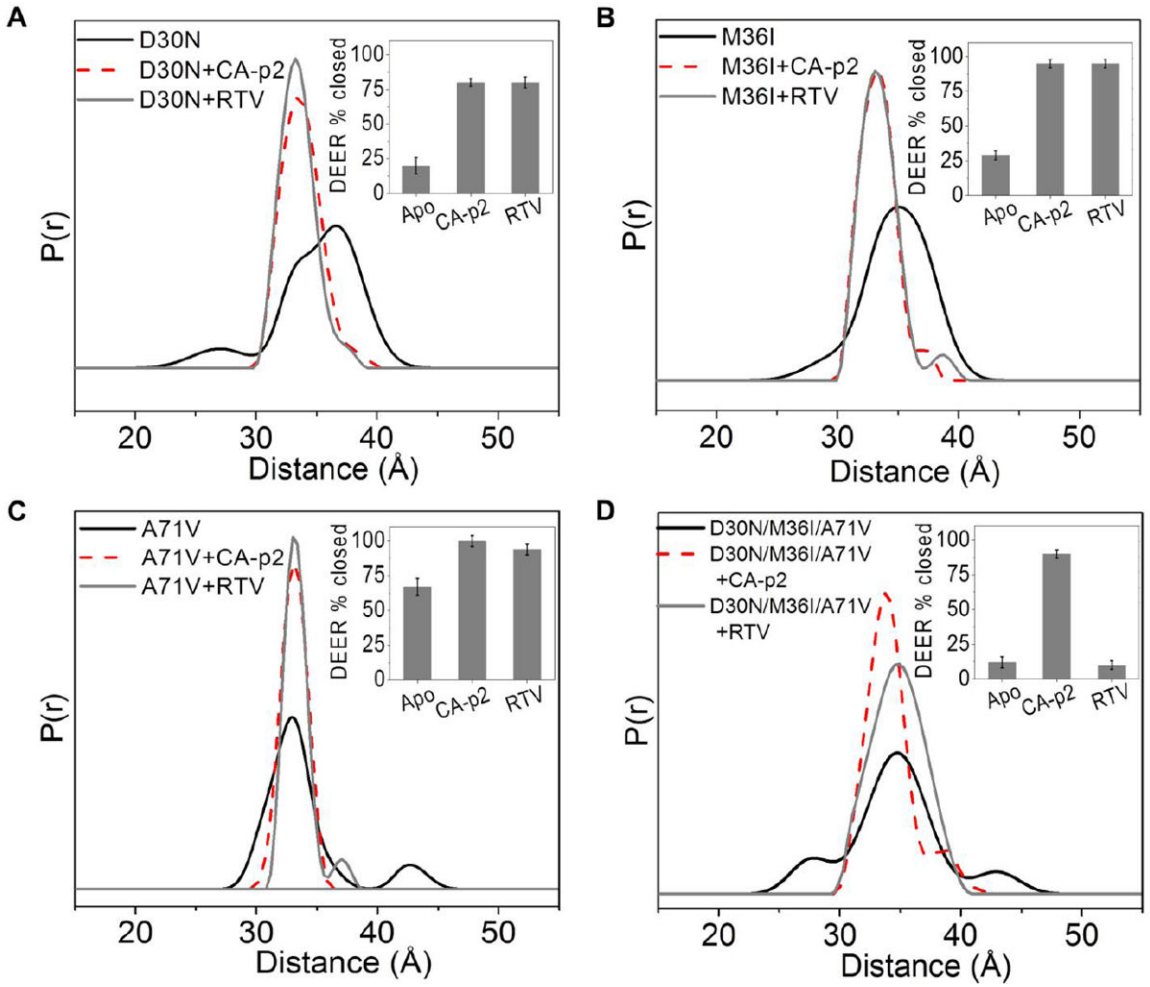

Figure 4.

Area-normalized distance profiles for apo (black), CA-p2-bound (red) and RTV-bound (blue) (A) D30N, (B) M36I, (C) A71V and (D) D30N/M36I/A71V HIV-1 protease constructs. Inset shows a bar graph of the relative percentage of the closed population from DEER analysis (DEER % closed) for apo and with CA-p2 substrate mimic or RTV.

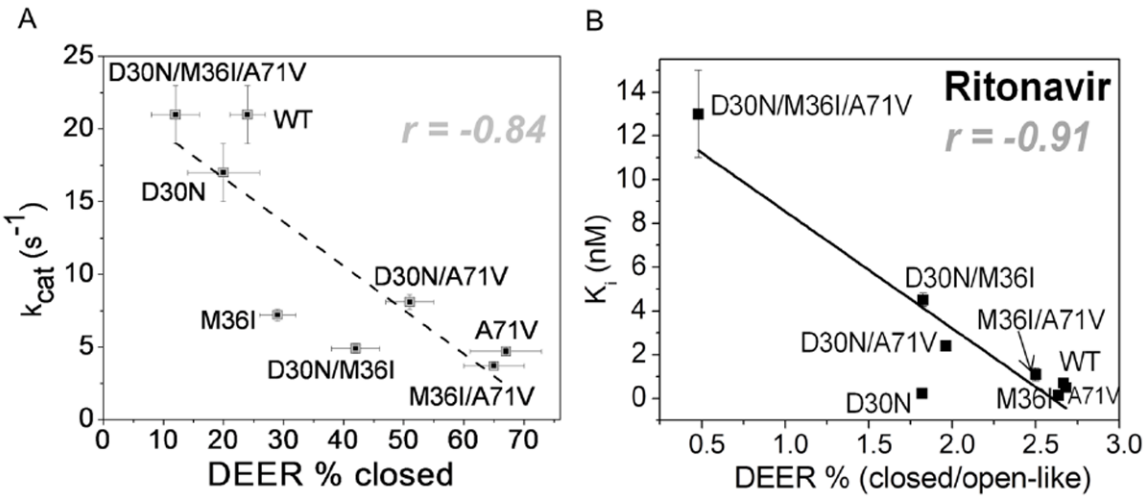

Figure 5.

Correlation plots for trends of DEER population percentages with kinetic and inhibition parameters. The Pearson product moment coefficient (*r*) is reported for each plot. (A) Percentage of closed population is inversely correlated to k_{cat}. (B) Percentage ratio of closed to open-like populations is inversely correlated to the inhibition constant (K_i) for ritonavir. Similar correlations are demonstrated using K_i of other inhibitors (see Supporting Information).

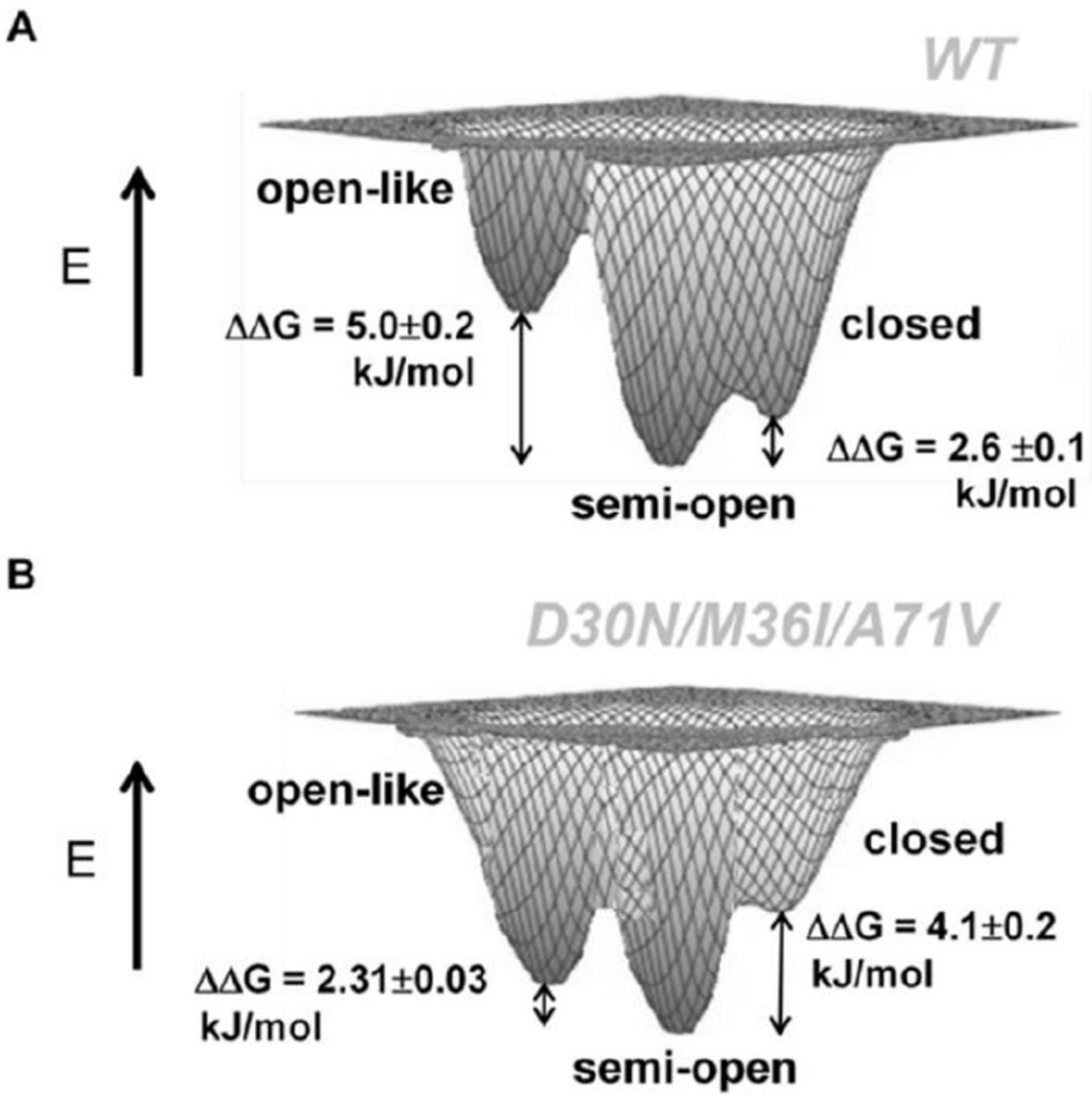

Figure 6.

Hypothetical thermodynamic profiles for (A) WT subtype B and (B) D30N/M36I/A71V variants. For each, the energy of the semi-open conformations are set equal and the relative free energy differences are calculated with respect to the semi-open conformation. Free energies were calculated directly from the relative percentages of DEER conformational populations, where the open-like percentage is the sum of the wide-open and curled/tucked states.

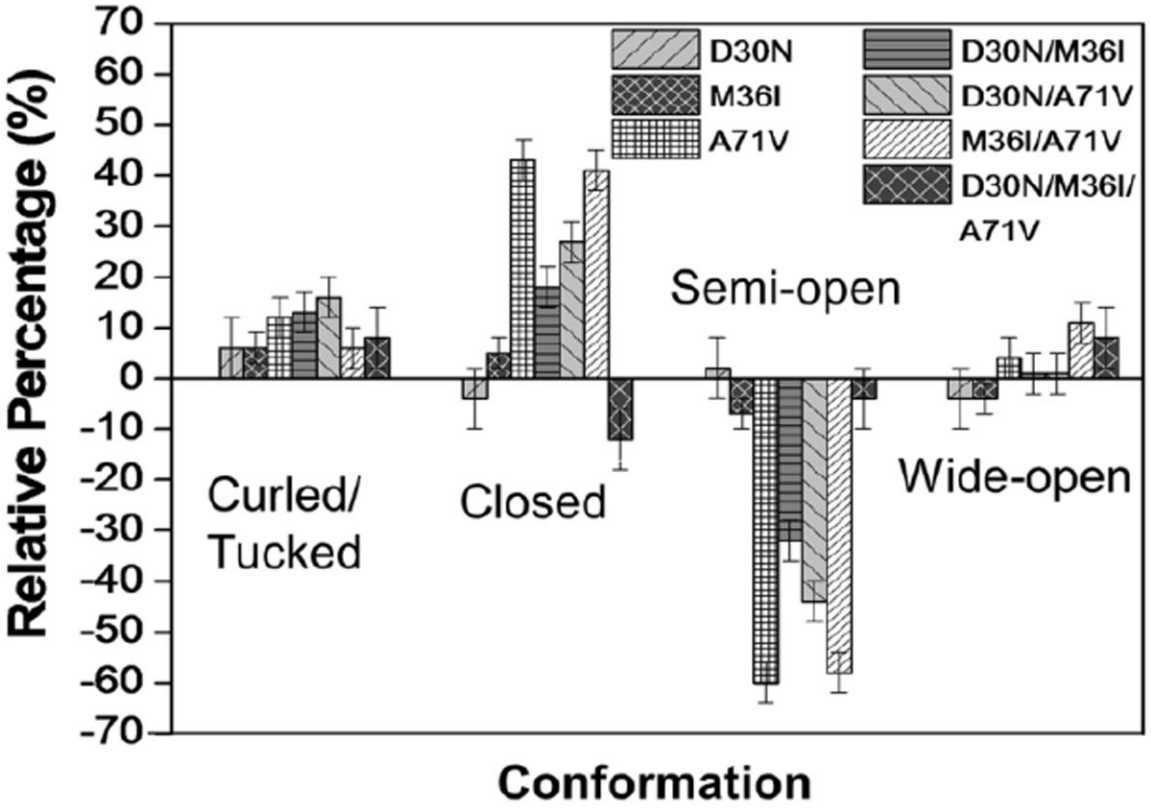

Figure 7.
Relative percentage change in the population of each conformation for the variants studied. The relative percentage change is calculated with respect to WT subtype B, % (P_i- P_{WT}).

Table 1

Summary of Pearson product moment coefficients (*r*) for DEER relative percentages correlated to inhibition constants (K_i)

	R		
Relative percentage of conformation from DEER	***K*i*** **(NFV)**	***K*i (RTV)**	***K*i (IDV)**
% semi-open	0.39	0.22	0.39
% wide-open	0.30	0.46	0.04
% open-like	0.28	0.44	0.24
%curled/tucked	0.12	0.17	0.32
%(semi-open/open-like)	-0.06	-0.23	-0.04
%(closed-like/semi-open)	-0.43	-0.31	-0.55
%(closed-like/wide-open)	-0.52	-0.55	-0.35
% closed-like-	-0.59	-0.44	-0.58
%(closed-like/open-like)	-0.98	-0.91	-0.95

* All *K*i values are from Clemente et al., 2003 [13]